Reversible Association of Calf Thymus Histones to Form the Symmetrical Octamer $(H2AH2BH3H4)_2$: A Case of a Mixed-Associating System†

Jamie E. Godfrey, Thomas H. Eickbush, and Evangelos N. Moudrianakis*

ABSTRACT: A mixture of calf thymus core histones, H2A, H2B, H3, and H4, dissolved in 2 M NaCl, pH 7.5, was analyzed by high-speed (meniscus depletion) equilibrium sedimentation at two different cell-loading concentrations. From analysis of apparent molecular weight vs. concentration profiles it is concluded that the core histones constitute a reversible, *mixed*-associating system leading to the formation of the symmetrical octamer $(H2AH2BH3H4)_2$:

$$H2AH2B + (H3H4)_2 \rightleftharpoons H2AH2B(H3H4)_2$$

$$H2AH2B + H2AH2B(H3H4)_2 \rightleftharpoons (H2AH2BH3H4)_2$$

The best fit to the data is obtained with both K_1 and K_2 equal to $(8.2 \pm 1.0) \times 10^5$ L/mol; the mild nonideality of the system can be described by a single virial coefficient, $B = 2.2 \times 10^{-7}$ (mol L)/g^2. A model for the core histone octamer featuring two identical and strongly cooperative binding sites on the H3–H4 tetramer for the H2A–H2B dimer is presented. Other modes of association were explored, including two containing a heterotypic tetramer, H2AH2BH3H4, but none gave as good a fit to the experimental data as did the hexamer intermediate model depicted above. Moreover, it is shown that the fitted model is consistent with results previously obtained from chromatographic studies on the core histones [Eickbush, T. H., & Moudrianakis, E. N. (1978) *Biochemistry 17*, 4955–4964]. Since few examples of mixed-associating as opposed to self-associating systems analyzed by equilibrium sedimentation have been described in the literature, several aspects of the mode-fitting procedure unique to such systems are discussed.

We have recently shown (Eickbush & Moudrianakis, 1978) that an octamer composed of two each of the core histones H2A, H2B, H3, and H4 is stable in 2 M salt at neutral pH. This species—with the same complement of histones found in the nucleosome (Kornberg, 1974)—appeared to be the product of a temperature-dependent association of two or more smaller species. Thomas & Butler (1977) and Chung et al. (1978) have also reported on the presence of a histone octamer in 2 M salt, and on the basis of equilibrium sedimentation experiments, the latter group has proposed that the octamer is in reversible equilibrium with 2 mol of the heterotypic tetramer, H2AH2BH3H4. Experimental results interpreted to suggest the existence of this tetrameric species under various solvent conditions have been published by a number of workers (Weintraub et al., 1975; Campbell & Cotter, 1976; Pardon et al., 1977; Wooley et al., 1977; Chung et al., 1978). However, our chromatographic studies which demonstrated the presence of the octamer in 2 M salt (Eickbush & Moudrianakis, 1978) produced no evidence for the presence of a heterotypic tetramer; if the octamer is formed from smaller species, it does not appear that a heterotypic tetramer is involved.

The present study was undertaken to identify the mode of association by which the core histone octamer is formed and to determine whether the several species involved are in chemical (reversible) equilibrium. We chose to study the association by equilibrium sedimentation; in addition to having a firm thermodynamic basis, this technique is particularly suited for the analysis of systems with a limited number (<5) of interacting species (Fujita, 1975; Teller et al., 1969; Adams & Filmer, 1966). Our studies reveal that the core histone octamer is the product of a mixed-association as opposed to a self-association (i.e., the association of dissimilar reactants) and that the association is reversible. Although several authors have addressed the sedimentation of mixed-associating systems from a theoretical standpoint (Nichol & Ogston, 1965; Adams, 1969; Chun & Kim, 1970), few (if any) examples of such systems analyzed by equilibrium sedimentation have been reported in the literature. For this reason, the analysis of the experimental data on the core histone system is described in some detail and a number of problems encountered in analyzing mixed systems are discussed.

Materials and Methods

Core Histones. Calf thymus histones were isolated as described previously (Eickbush & Moudrianakis, 1978). When chromatographed at 4 °C on a Sephadex G-100 column equilibrated with 2 M NaCl and 0.01 M Tris-HCl, pH 7.5, a mixture of histones H2A, H2B, H3, and H4 eluted as a single peak (shaded area, Figure 1A) which we have called the "core-complex" peak. From sodium dodecyl sulfate ($NaDodSO_4$)–urea–acrylamide disc gel electrophoresis (Eickbush & Moudrianakis, 1978) and Bio-Rad P-60 chromatography (Figure 1B), the relative mass concentrations of the four histones in the core-complex peak were found to be H2A/H2B/H3/H4 = 1.00:1.02:1.47:1.11. On a molar basis, this ratio is H2A/H2B/H3/H4 = 1.00:1.04:1.34:1.38. The molecular weight values for the four histones reported by DeLange et al. (1969), Delange et al. (1973), Candido & Dixon (1972), and Yeoman et al. (1972) were used in determining the latter ratio (H2A = 14 004 g/mol; H2B = 13 774 g/mol; H3 = 15 324 g/mol; H4 = 11 282 g/mol). The peak contains no other protein in significant concentration.[1] Because of its elution position (close to where an octamer of 108 000 molecular weight would be expected to appear), the core-complex peak only contains protein capable of associating

† Contribution No. 1049 from the Department of Biology, The Johns Hopkins University, Baltimore, Maryland 21218. *Received May 2, 1979; revised manuscript received August 30, 1979.* A summary of this work was presented at the 22nd Annual Meeting of the Biophysical Society, held in Washington, D.C., March 27–30, 1978, Abstract No. TU-AM-H15. This work was supported in part by a Biomedical Research Support Grant from the National Institutes of Health and by the American Cancer Society and in part by Grant No. AM-04349 from the National Institutes of Health to Dr. W. F. Harrington.

[1] A trace (less than 2% of the total protein) of histone A24 can be seen on the $NaDodSO_4$ gels. As will be shown in a subsequent report, this histone, which is a modified form of H2A, has similar association properties.

0006-2960/80/0419-1339$01.00/0

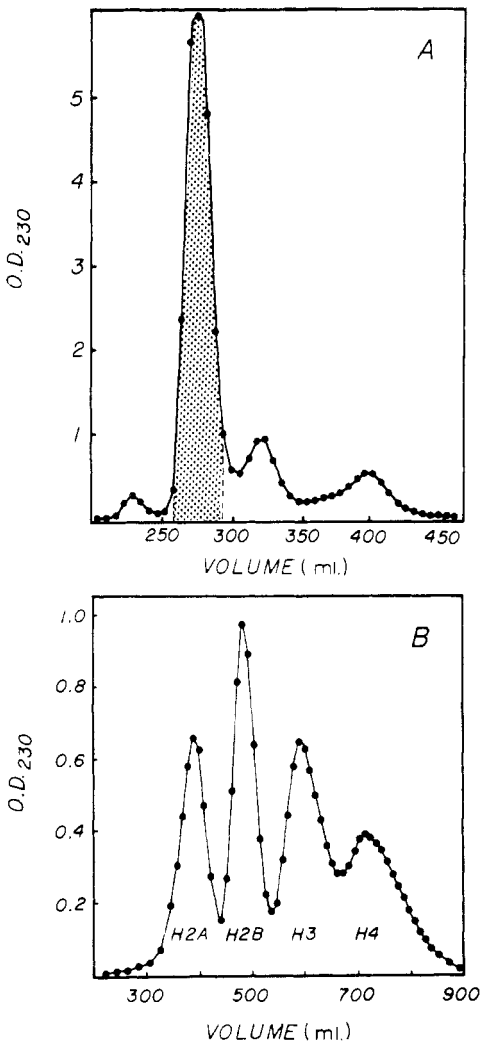

FIGURE 1: (A) Sephadex G-100 column fractionation of histone complexes extracted from calf thymus chromatin with 2 M NaCl and 10 mM Tris-HCl, pH 7.5, at 4 °C. Shaded area is the core-complex peak [from Figure 1 in Eickbush & Moudrianakis (1978)]. (B) Bio-Rad P-60 fractionation of the core-complex peak proteins. A 2.5 × 130 cm column equilibrated with 0.01 M HCl was loaded with 60 mg of protein from the core-complex peak previously dialyzed against the equilibrating buffer and eluted at 4 °C with the equilibrating buffer. Areas under peaks were estimated from Gaussian curve fitting and normalized for the differences in the absorbancies of the four core histones at 230 nm. Relative concentrations of H3 and H4 were estimated by $NaDodSO_4$–urea–acrylamide gel electrophoresis (Eickbush & Moudrianakis, 1978).

to larger species. We chose, therefore, to analyze the peak histone mixture "as is" rather than titrate it to equal molarity with H2A and H2B, since we could not be sure that all of the added histone would be competent to interact. Histone concentrations were routinely measured by the biuret method, calibrated for the four histones, as described in Eickbush & Moudrianakis (1978).

Analytical Ultracentrifugation. Equilibrium sedimentation experiments at rotor speeds causing meniscus depletion (Yphantis, 1964) were performed in a Beckman Model E analytical ultracentrifuge equipped with Rayleigh interference optics and the Electronic Speed Control unit. The camera lens was focused on the two-thirds level of the cell to minimize Weiner skewing (Yphantis, 1964). For all experiments the histone mixture was dialyzed against 2 M NaCl and 0.01 M Tris-HCl, pH 7.5, at 20 °C. In this solvent the histone mixture has a density increment, $(\partial \rho/\partial c)_{u,T,P}$, of 0.189; this value is based on our previously reported value for the partial volume ($\phi' = 0.753$ mL/g; Eickbush & Moudrianakis, 1978) in this buffer measured under conditions of dialysis equilibrium (Eisenberg, 1976).

Double-sector cells fitted with 12-mm aluminum-filled epon centerpieces and quartz windows were filled to a column height of 2.7 mm (100 μL) with protein solution and dialysate. In a typical experiment, a regular and two wedge cells (0.6° up and down) were run in an An-F (four-hole) aluminum rotor. At the rotor speed used (26 000 rpm; no overspeeding) sedimentation equilibrium was attained in 24 h or less, as evidenced by constant Rayleigh patterns over 8-h intervals. dn/dc for the core-complex proteins was determined by the synthetic boundary cell method (Chervenka, 1973) to allow fringe displacements to be converted to units of milligrams per milliliter. Further details of procedures followed (e.g., blank runs, plate reading, data reduction) can be found in Godfrey & Harrington (1970) and Godfrey (1976). Apparent number-, weight-, and z-average molecular weights were generated with the aid of the computer program written by Roark & Yphantis (1969).

Results

Results from chromatographic studies and preliminary equilibrium sedimentation experiments (Eickbush & Moudrianakis, 1978) had suggested to us that the core-complex peak histones associate reversibly in 2 M NaCl. An octamer containing 2 mol each of the four histones clearly seemed to be in equilibrium with two or more smaller species. Moreover, the system was found to be decidedly sensitive to temperature. With increasing temperature, the equilibrium is shifted from the high molecular species toward lower weight intermediates. On the basis of these observations, we chose to make a detailed study of the system at 20 °C since at this temperature it appeared likely that all of the species involved in the reversible association would be present in measurable concentrations. Results from experiments with a low cell-loading concentration are presented first; these data are then fitted to what we believe to be the most likely association mode; next, data from runs with a higher cell-loading concentration are analyzed to demonstrate that the association is indeed reversible; last, alternative schemes of association are considered.

Figure 2 shows the apparent number-, weight-, and z-average molecular weights for the core-complex histones at 20 °C as a function of total protein concentration. The points are averaged values from six runs at 26 000 rpm and a cell-loading concentration of 0.35 mg/mL. The solid curves "through" the data points were generated by the fitted model described below. Under the run conditions employed, there was no detectable packing of material on the cell bottom (c_b was ~2.5 mg/mL). Nor was solute retained at the meniscus at sedimentation equilibrium as evidenced by the presence of a gradient-free region of ~800 μm at the top of the solution column (see Discussion).

After attempts with other association modes (see below), we successfully fitted the data to the scheme

$$\mathrm{H2A} + \mathrm{H2B} \rightleftharpoons \mathrm{H2AH2B} \quad (1a)$$

$$2\mathrm{H3} + 2\mathrm{H4} \rightleftharpoons \text{intermediates } (?) \rightleftharpoons (\mathrm{H3H4})_2 \quad (1b)$$

$$\mathrm{H2AH2B} + (\mathrm{H3H4})_2 \rightleftharpoons \mathrm{H2AH2B(H3H4)_2} \quad (2a)$$

$$K_1 = [\text{hexamer}]/([\text{dimer}][\text{tetramer}])$$

$$\mathrm{H2AH2B} + \mathrm{H2AH2B(H3H4)_2} \rightleftharpoons (\mathrm{H2AH2BH3H4})_2 \quad (2b)$$

$$K_2 = [\text{octamer}]/([\text{dimer}][\text{hexamer}])$$

In agreement with previously reported observations (D'Anna

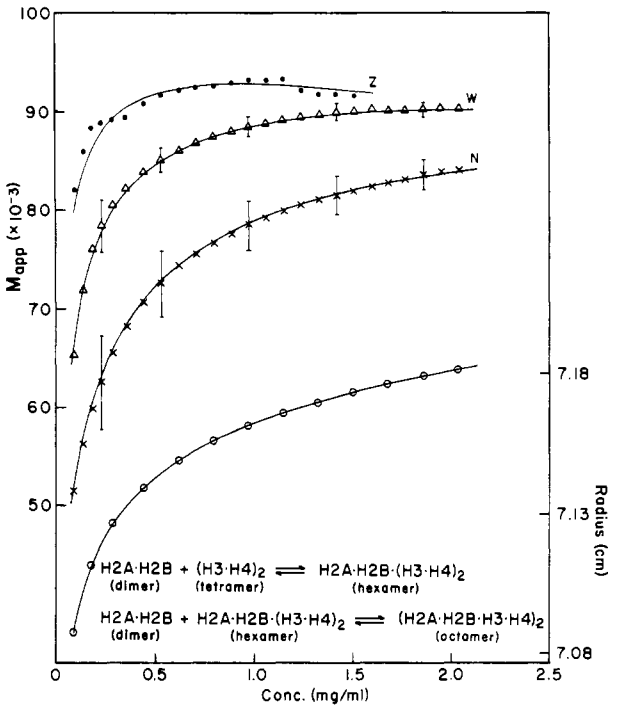

FIGURE 2: Meniscus depletion equilibrium sedimentation of the core-complex histones in 2 M NaCl and 10 mM Tris-HCl, pH 7.5, at 20 °C. Apparent number-average (×), weight (Δ), and z-average (●) molecular weights plotted vs. solute concentration ($\bar{c}_r$). Radius (○) vs. $\bar{c}_r$ is also shown. Data points are averaged from six runs made under identical conditions; error bars are ±85% confidence limits. Other run conditions: 0.35 mg/mL cell loading; 26 000 rpm. Curves are the corresponding apparent averages and radii vs. $\bar{c}_r$ obeying the hexamer intermediate model (eq 2a and 2b); for values of K_1, K_2, and B, see Figure 6.

& Isenberg, 1974a,b; Roark et al., 1974, 1976), the equilibria shown in eq 1a and 1b are assumed to be strongly in favor of the right-hand products under the experimental conditions used—so much so that none of the monomer species nor possible intermediates leading to the formation of the H3–H4 tetramer are present in detectable concentrations. The two equilibria shown in eq 2a and 2b show the octamer in equilibrium with the tightly bound H2A–H2B dimer and H3–H4 tetramer through a hexamer intermediate. The system is characterized by the two molar association constants, K_1 and K_2.

In fitting the data to this mode, it was assumed (a) that any nonideal behavior of the system can be adequately described by a single concentration-independent virial coefficient applicable to all species (i.e., $\ln y_i = BM_i\bar{c}$) (Adams & Fujita, 1963; Teller, 1973), (b) that pressure effects are absent (Harrington & Kegeles, 1973) [i.e., $(\partial\rho/\partial c)_{u,T}$ is constant within the range of hydrostatic pressures generated by the experiment], and (c) that $(\partial\rho/\partial c)_{u,T,P}$ for any of the species present does not differ significantly from the average value measured for the core-complex mixture (Nichol & Ogston, 1965; Adams, 1969). In addition, the molar concentration ratio for the four histones, H2A/H2B/H3/H4, was taken to be 1.00:1.00:1.33:1.33 (see Materials and Methods) since the model (eq 2a and 2b) assumes equimolar amounts of H2A and H2B and equimolar amounts of H3 and H4. On a mass basis, (H2A + H2B)/(H3 + H4) = 1.00:1.28.

Because this is a system of mixed-association (not of self-association), conservation of the mass of each of the reactants must be observed in the mode-fitting procedure (Nichol & Ogston, 1965). For the mode described by eq 2a and 2b, the following mass balances hold

$$Q_{3+4} = 1.28Q_{2A+2B} \quad (3)$$

$$Q_{2A+2B} = Q_D + (M_D/M_H)Q_H + (2M_D/M_O)Q_O \quad (4)$$

$$Q_{3+4} = Q_T + (M_T/M_H)Q_H + (M_T/M_O)Q_O \quad (5)$$

where Q and M are mass and molecular weight, respectively, the subscripts 2A, 2B, 3, and 4 refer to the four histones, and the subscripts D, T, H, and O refer, respectively, to the dimer, tetramer, hexamer, and octamer species. The mass of an ideal-behaving solute (in milligrams), Q_i, at sedimentation equilibrium in a sector-shaped cell can be expressed in terms of its concentration (in milligrams per milliliter) at any radial position, r_a, by

$$Q_i = \int_{r_m}^{r_b} \Theta c_i r \, dr = \frac{\Theta c_{i(r_a)}}{2\phi M_i}[\exp[\phi M_i(r_b^2 - r_a^2)] - \exp[\phi M_i(r_m^2 - r_a^2)]] \quad (6)$$

where Θ incorporates cell dimensional constants and ϕ is $\omega^2(\partial\rho/\partial c)_{u,T,P}/2RT$ (Nichol & Ogston, 1965); other symbols have their usual definitions. Although eq 6 applies only to ideal systems, we believe that this relationship is also a very good approximation for moderately nonideal-behaving systems if r_a is chosen at a point near the center of mass of the protein distribution (see Discussion). Combining eq 2–6 leads to the following relationship between the concentrations of H2A–H2B dimer (D_{r_a}) and H3–H4 tetramer (T_{r_a}) at r_a

$$T_{r_a} = A_1 D_{r_a}/(A_2 + A_3k_1D_{r_a} + A_4k_1k_2D_{r_a}^2) \quad (7)$$

where k_1 and k_2 are the association constants for equilibria 2a and 2b in mass units (milliliters per milligram). A_1–A_4 are constants; under the conditions used and with r_a equal to 7.14 cm, they are respectively 0.079, 0.058, 0.0151, and −0.0153.

The total protein concentration at r_a is known (the average value from the six runs), and since it is the sum of the several species

$$\bar{c}_{r_a} = D_{r_a} + T_{r_a} + H_{r_a} + O_{r_a} = D_{r_a} + T_{r_a} + k_1D_{r_a}T_{r_a} + k_1k_2D_{r_a}^2T_{r_a} \quad (8)$$

eq 7 can be rewritten in a form eliminating T_{r_a}:

$$D_{r_a} = \frac{\bar{c}_{r_a}(A_2 + A_3k_1D_{r_a} + A_4k_1k_2D_{r_a}^2)}{A_1(1 + k_1D_{r_a} + k_1k_2D_{r_a}^2) + A_2 + A_3k_1D_{r_a} + A_4k_1k_2D_{r_a}^2} \quad (9)$$

This equation defines sets of values for D_{r_a}, k_1, and k_2 which preserve the known mass ratio between the histones in the cell. Corresponding values for the concentrations of tetramer, hexamer, and octamer at r_a can be obtained with eq 7 and 8.

Concentrations of each of the species as a function of radial position can be generated from eq 10 (Nichol & Ogston, 1965; Milthorpe et al., 1975) by assuming a value for B (see below). $\sum c_{i(r_a)}$ and $\sum c_{i(r)}$ are approximated by the averaged experimental values $\bar{c}_{r_a}$ and $\bar{c}_r$ to avoid a complex iterative process. This procedure yields correct concentration distributions for each of the species at sedimentation equilibrium if the model fits the experimental data (i.e., if the sum of the concentrations of all species calculated from eq 10 equals the experimental value for the total concentration throughout the cell).

$$c_{i(r)} = c_{i(r_a)} \exp[BM_i[(\sum c_{i(r_a)} - \sum c_{i(r)}) + \phi M_i(r^2 - r_a^2]] \quad (10)$$

With the aid of a computer, apparent number-, weight-, and z-average molecular weights were generated as a function of total protein concentration for different sets of values of D_{r_a},

k_1, and k_2 as defined by eq 9 and several values of B within realistic (positive) limits (Teller, 1973). These theoretical distributions were calculated from the concentrations of each of the species as a function of radial position (eq 10) and the definitions of the three moments:

$$1/M_{n(app)(r)} = 1/M_{n(r)} + B\sum c_{i(r)}/2 = [(\sum c_{i(r)}/M_i)/\sum c_{i(r)}] + B\sum c_{i(r)}/2$$

$$1/M_{w(app)(r)} = 1/M_{w(r)} + B\sum c_{i(r)} = (\sum c_{i(r)}/\sum c_{i(r)}M_i) + B\sum c_{i(r)}$$

$$1/M_{z(app)(r)} = 1/M_{z(r)} + 2B\sum c_{i(r)}(M_{w(r)}/M_{z(r)}) + [B\sum c_{i(r)}(M_{w(r)}/M_{z(r)})]^2 \simeq (\sum c_{i(r)}M_i/\sum c_{i(r)}M_i^2)(1 + 2B\sum c_{i(r)}M_{w(r)})$$

The best fit was obtained with k_1 = 45 L/mol and k_2 = 40 L/mol and a value of 2.2×10^{-7} (mol L)/g^2 for B. The corresponding molar association constants, K_1 and K_2, are both equal to 8.2×10^5 L/mol. The solid curves in Figure 2, which closely approximate the data points, are apparent molecular weight moments generated by the model with these values for K_1, K_2, and B. The lowest curve in Figure 2 is the total concentration plotted against the radial position; again the points are averaged data from the six runs, and the solid curve is generated by the model. It can be seen that $\sum c_{i(r)}$ superimposes on $\bar{c}_r$, thereby fulfilling the requirement imposed on eq 10, if $\bar{c}_r$ is substituted for $\sum c_{i(r)}$.

From numerical integration of curves generated by eq 10, it was found that the fitted model yields a mass ratio between the histones identical with the closely approximated value used in the fitting process: (H2A + H2B)/(H3 + H4) = 1.00:1.28. This demonstrates the applicability of eq 6 to this nonideal system when r_a is chosen at a point close to the center of mass.

Several runs were made at a significantly higher cell-loading concentration to test whether the core histones are in reversible equilibrium. Figure 3 presents apparent number- and weight-average molecular weight distributions (solid symbols) as a function of total solute concentration averaged from three experiments at a rotor speed of 26 000 rpm and a cell loading of 2.0 mg/mL. As was observed with the runs at the 0.35 mg/mL cell-loading concentration, these runs exhibited a gradient-free region (~400 μm) at the centripetal end of the solution column indicative of solute depletion at the meniscus. For comparison, the apparent number and weight results from the six runs at the lower cell-loading concentration (Figure 2) are also shown (open symbols), along with the distributions generated by the fitted model (closely approximating solid curves). Although the two sets of data are similar, they do not superimpose as would be required for a self-associating system (Adams & Fujita, 1963; Yphantis, 1964). However, except for a limited number of cases, mixed-associating systems do not obey this rule, rather they will generally exhibit some limited displacement of their apparent molecular weight average curves in response to changing run conditions. Following the procedure outlined above, apparent weight- and number-average molecular weight distributions for the fitted model were generated by assuming the higher (2.0 mg/mL) cell-loading concentration. As expected, these curves do not superimpose on the theoretical distributions for the lower cell-loading condition, but they do closely approximate the experimental data points from the three runs at the higher loading concentration.

As further evidence of the reversibility of the histone system, it is useful to compare the experimental data with results expected from a hypothetical mixture of nonreversible aggregates of the four histones. For example, what would be

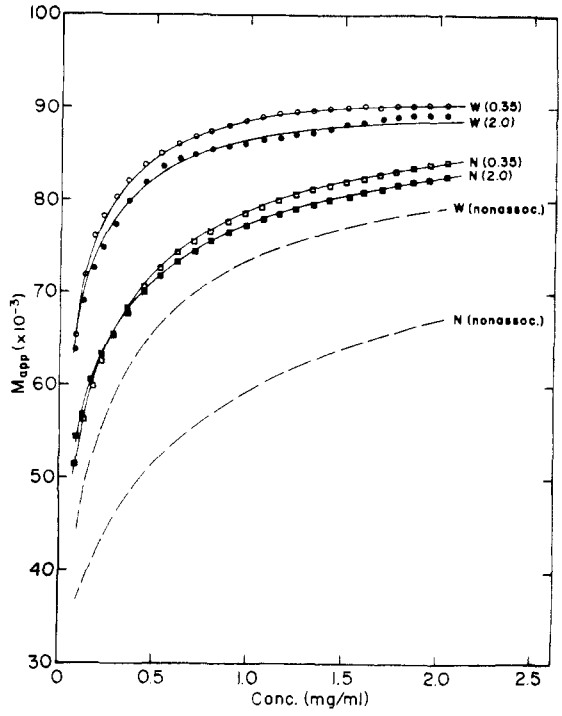

FIGURE 3: Meniscus depletion equilibrium sedimentation of the core-complex histones at two different cell-loading concentrations. Apparent number-average (squares) and weight-average (circles) molecular weights plotted vs. solute concentration ($\bar{c}_r$). Open symbols are from six runs at a cell loading of 0.35 mg/mL (from Figure 2); solid symbols are averaged from three runs at a cell loading of 2.0 mg/mL. Other conditions for the two sets of runs were identical: 2 M NaCl and 10 mM Tris-HCl, pH 7.5; 26 000 rpm; 20 °C. Solid curves are the corresponding apparent averages obeying the fitted model (eq 2a and 2b); for values of K_1, K_2, and B, see Figure 6. Dashed curves are apparent number-average (N) and weight-average (W) molecular weight distributions expected at the higher (2.0 mg/mL) cell-loading concentration for a nonreversible mixture of dimer, tetramer, hexamer, and octamer which would approximate the fitted model curves at the lower (0.35 mg/mL) cell-loading concentration.

expected at the higher cell-loading concentration (2.0 mg/mL) if the system were a mixture of four noninteracting species, dimer, tetramer, hexamer, and octamer, which would give rise to the molecular weight distributions measured at the lower (0.35 mg/mL) loading concentration? In general, the molecular weight averages of heterodisperse systems shift to significantly lower values if the cell-loading concentration is increased fivefold or more when the averages are plotted as a function of total solute concentration (Yphantis, 1964). This is the case for the nonassociating mixture proposed above. The dashed curves in Figure 3 are the apparent weight- and number-average molecular weight distributions for such a system if it were run at the higher cell-loading concentration. It seems highly unlikely, therefore, that the results obtained with the core-complex proteins at the two cell-loading concentrations were generated by a mixture of noninteracting histone aggregates.

In addition to the successful hexamer intermediate model, other association modes were evaluated. One mode given serious consideration is depicted in eq 11 and 12, which show an octamer species in equilibrium with a heterotypic tetramer intermediate.

$$\text{H2AH2B} + \text{H3H4} \rightleftharpoons \text{H2AH2BH3H4} \qquad (11)$$

$$K_1 = [\text{tetramer}]/([\text{H2A–H2B dimer}][\text{H3–H4 dimer}])$$

$$2(\text{H2AH2BH3H4}) \rightleftharpoons (\text{H2AH2BH3H4})_2 \qquad (12)$$

$$K_2 = [\text{octamer}]/[\text{tetramer}]^2$$

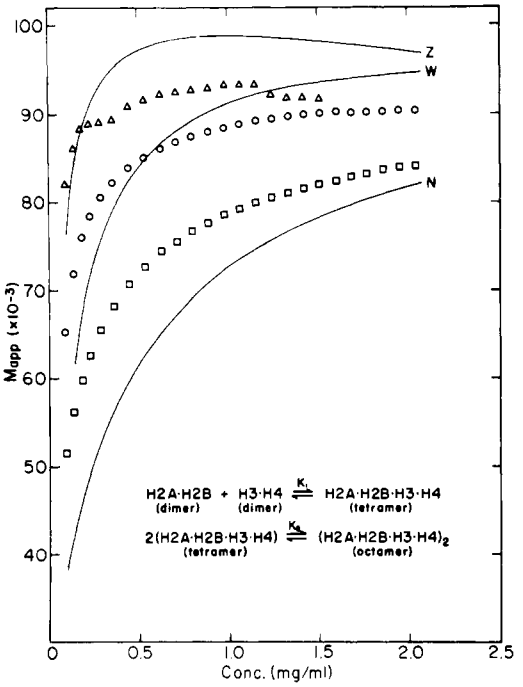

FIGURE 4: Best fit to the experimental data obtained with the heterotypic tetramer model. Apparent number-average (□), weight-average (○), and z-average (△) molecular weights for the set of runs at the lower (0.35 mg/mL) cell-loading concentration plotted vs. solute concentration ($\bar{c}_r$) (from Figure 2). Curves are the number-average (N), weight-average (W), and z-average (Z) moments obeying the heterotypic tetramer mode (eq 11 and 12); for values of K_1, K_2, and B, see Results.

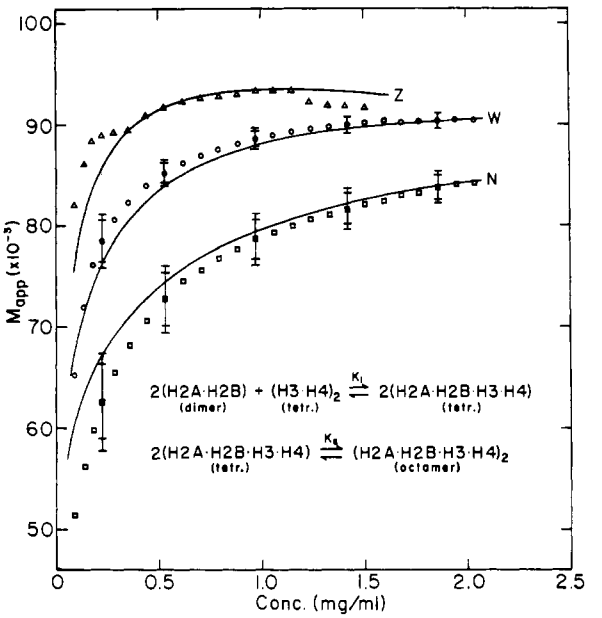

FIGURE 5: Best fit of the experimental data to a variation of the heterotypic tetramer model (i.e., H3–H4 tetramer/heterotypic tetramer). Apparent number-average (□), weight-average (○), and z-average (△) molecular weights for the set of runs at the lower (0.35 mg/mL) cell-loading concentration plotted vs. solute concentration ($\bar{c}_r$) (from Figure 2). Curves are number-average (N), weight-average (W), and z-average (Z) moments obeying the H3–H4 tetramer/heterotypic tetramer mode (eq 13 and 12); for values of K_1, K_2, and B, see Results. Outer error bars are 85% confidence limits; inner bars are 75% confidence limits.

Several workers have reported results suggesting the existence of the heterotypic tetramer species in core histone preparations under a variety of conditions (Weintraub et al., 1975; Campbell & Cotter, 1976; Chung et al., 1978; Pardon et al., 1977; Wooley et al., 1977). Figure 4 shows the best fit to the experimental results we could obtain with this mode [$K_1 = 3.3 \times 10^6$ L/mol; $K_2 = 1.8 \times 10^6$ L/mol; $B = 2.0 \times 10^{-7}$ (mol L)/g^2]. Values for K_1, K_2, and B can be chosen to allow a close fit between model and data for one of the molecular weight averages, but this results in even poorer fits to the other two averages than any depicted in Figure 4. No better fit is obtained when it is assumed that only octamer and heterotypic tetramer are present in 2 M NaCl (i.e., K_1 is infinite), as Chung et al. (1978) have done in a recent report (see Discussion).

A closer fit to the data was obtained when eq 11 was replaced with an alternative mechanism for forming the heterotypic tetramer (Figure 5):

$$2(\text{H2AH2B}) + (\text{H3H4})_2 \rightleftharpoons 2(\text{H2AH2BH3H4}) \quad (13)$$

$$K_1 = [\text{hetero tetramer}]^2/([\text{H2A–H2B dimer}]^2[\text{H3–H4 tetramer}])$$

$$2(\text{H2AH2BH3H4}) \rightleftharpoons (\text{H2AH2BH3H4})_2 \quad (12)$$

$$K_2 = [\text{octamer}]/[\text{hetero tetramer}]^2$$

In this scheme, both H3–H4 tetramer and heterotypic tetramer are assumed to be present and in equilibrium with each other; in line with published evidence (see above), this mechanism avoids postulating the presence of H3–H4 dimer and is, therefore, perhaps more realistic than the model described by eq 11 and 12.[2] However, this mechanism requires that the two experimentally identifiable subunits of the core histones, i.e., the H2A–H2B dimer and the H3–H4 tetramer, first bind and then rearrange their interactions to yield two heterotypic tetramers. To our knowledge there is no experimental evidence to support such a rearrangement within the histone subunits; thus, this mechanism is at present entirely speculative. This mode fits the three experimental molecular weight moments reasonably well at high concentrations but deviates significantly at concentrations below 0.8 mg/mL [$K_1 = 1.13 \times 10^8$ L/mol; $K_2 = 6.9 \times 10^5$ L/mol; $B = 2.6 \times 10^{-7}$ (mol L)/g^2]. The superior fit of the hexamer intermediate model over this model is reflected in a comparison of their respective root mean square deviations from the experimental data. The values for the H3–H4 tetramer–heterotypic tetramer model (eq 13 and 12) are 3000, 1300, and 2200 daltons for the apparent number, weight, and z averages, respectively; for the hexamer intermediate model, they are 340, 430, and 1000 daltons.

More complex association modes involving additional intermediates and multiple end products could conceivably give closer fits to the data than can be obtained with the heterotypic tetramer models depicted in eq 11–13. However, no other mode which we have considered, regardless of complexity, gives a better fit to the experimental data than the hexamer intermediate model we have proposed.

The hexamer intermediate model gives the best fit to the data with $K_1 = K_2 = 8.2 \times 10^5$ L/mol. Satisfactory results can also be obtained with dissimilar values for the association

[2] The reaction depicted in eq 13 would likely involve a short-lived H3–H4 dimer intermediate which would quickly react with a second H2A–H2B dimer to form the second heterotypic tetramer:

$$\text{H2AH2B} + (\text{H3H4})_2 \rightleftharpoons \text{H2AH2BH3H4} + \text{H3H4 (trace)}$$

$$\text{H2AH2B} + \text{H3H4 (trace)} \rightleftharpoons \text{H2AH2BH3H4}$$

These two equilibria combine to give eq 13.

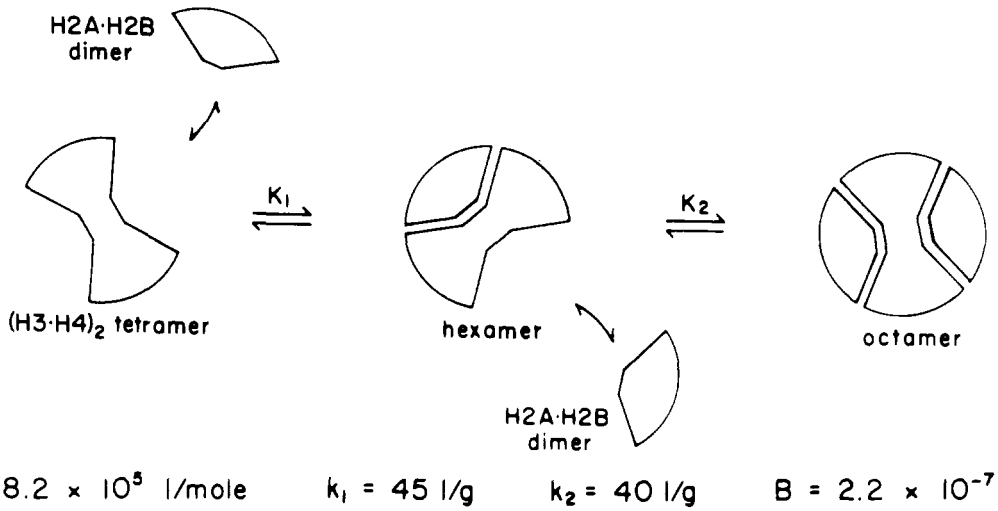

FIGURE 6: Hexamer intermediate model for the formation of the core histone octamer (eq 2a and 2b). The H3–H4 tetramer is shown with two identical binding sites, the model preferred by the authors (see Discussion). Values listed for the association constants (K_1 and K_2) and virial coefficient (B) gave the best fit to the experimental data. k_1 and k_2 are the corresponding association constants in mass concentration units.

constants, if they depart (each in the opposite sense) from the fitted value by no more than 10–15%. However, when values are chosen which differ by more than this amount, significant deviations from the data are seen. For example, with K_1 and K_2 equal to 9.8×10^5 and 6.6×10^5 L/mol, respectively (K_1/K_2 = 3:2), a reasonably good fit is obtained to the apparent weight-average molecular weight data at total protein concentrations below ~0.8 mg/mL; but at higher concentrations, the model values fall below the data and outside of the confidence limits depicted in Figure 2. Model and experimental values for the apparent number-average molecular weight differ as well. In this case, the model values are higher than the experimental values over the entire concentration range. [For the purpose of these calculations, B was assumed to be the fitted value 2.2×10^{-7} (mol L)/g^2.] We conclude, therefore, that K_1 and K_2 are equal to $(8.2 \pm 1.0) \times 10^5$ L/mol, by which it is understood that departures from 8.2×10^5 L/mol must obey (roughly) the relationship $(K_1 + K_2)/2 = 8.2 \times 10^5$ L/mol.

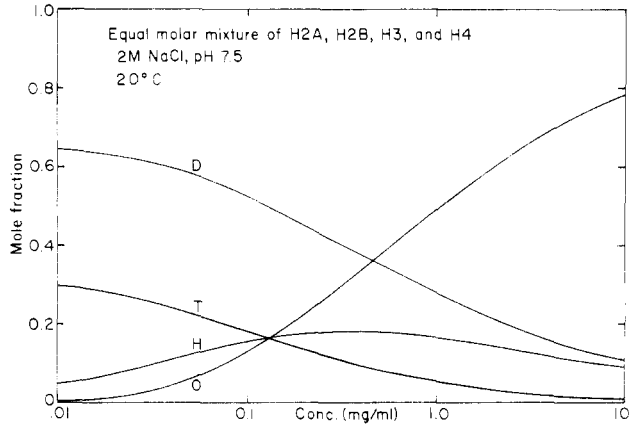

FIGURE 7: Mole fractions of dimer (D), tetramer (T), hexamer (H), and octamer (O) vs. total histone concentration (log scale) for an equal molar mixture of the core histones in 2 M NaCl, pH 7.5, at 20 °C. Distributions were calculated from the hexamer intermediate model (eq 2a and 2b) and values for K_1 and K_2 which gave the best fit to the experimental data (see Figure 6).

Discussion

We have presented evidence from high-speed equilibrium sedimentation experiments for the presence of a reversible association between the H2A–H2B dimer and H3–H4 tetramer in 2 M salt at neutral pH. Two products are formed; 1 mol each of dimer and tetramer associates to form the asymmetric hexamer, H2AH2B(H3H4)$_2$, and a second mole of dimer can add to the hexamer to form the symmetrical octamer, (H2AH2BH3H4)$_2$. The evidence suggesting a high degree of symmetry for the nucleosome (Felsenfeld, 1978) argues in favor of two identical binding sites on the tetramer (Figure 6). If this is indeed the case, a pronounced positive cooperativity between the sites must be present since K_1 and K_2 were calculated to be nearly equal in value; the binding of the first dimer to one site of the tetramer enhances by a factor of about 4 the intrinsic binding affinity of the second dimer at the remaining site (Hill coefficient = 1.32).[3] The presence of an allosteric link between the two sites is an attractive hypothesis for the basis of the observed cooperativity. It is worth noting in this regard that under conditions of high salt and neutral pH, the interaction of histones H2B and H4 results in an almost twofold increase in the total α-helix content of the system (D'Anna & Isenberg, 1973; Glover & Gorovsky, 1978). We are currently attempting to clarify this question.

Although the presence of two identical dimer binding sites on the H3–H4 tetramer is an attractive model, the data lend themselves to alternative interpretations. A variety of schemes involving nonidentical sites on the tetramer, binding between the H2A–H2B dimers, etc., can be formulated.

Under the experimental conditions employed, the octamer is the dominant species at concentrations of total protein above 1 mg/mL (Figure 7). Only at concentrations below 0.1 mg/mL is hexamer favored over octamer, and at these low concentrations the reactants, dimer and tetramer, are present at higher concentrations than either product. This general profile—hexamer never becoming the major constituent at any protein concentration—is independent of solvent conditions (as long as the two association constants remain nearly equal in value); changing the affinity of the H2A–H2B dimer for the H3–H4 tetramer in essence only shifts the abscissa in Figure 7 in one direction or the other.

At lower temperatures, the association appears to be greatly strengthened, so much so that at 4 °C the weight-average

[3] For completely independent sites, K_1 would have to be 4 times larger than K_2 due to the probabilities involved in filling two identical sites (Wold, 1971).

molecular weight for the core complex remains close to the octamer value (108 000) even at concentrations in the 0.1 mg/mL range (Eickbush & Moudrianakis, 1978). Evidence that the core histones form the symmetrical octamer at low temperature was first reported by Thomas & Butler (1977); it is interesting to note that these workers found almost the same nonideality [$B = 2.0 \times 10^{-7}$ (mol L)/g^2] for the system at 6 °C as we found at 20 °C.

Several laboratories have reported evidence for the presence of a heterotypic tetramer, H2AH2BH3H4, in core histone preparations in 2 M salt (Weintraub et al., 1975; Campbell & Cotter, 1976; Chung et al., 1978; Wooley et al., 1977; Pardon et al., 1977). Recently, Chung et al. (1978) have concluded from low-speed equilibrium sedimentation studies that the heterotypic tetramer associates reversibly to form the symmetrical octamer in 2 M NaCl, pH 9.0. Our results do not support this mechanism. The two-species mode (eq 12) gives a very poor fit to the data; the fit does not improve significantly when the mode is expanded to allow the dissociation of the heterotypic tetramer into two dimeric species (eq 11; Figure 4).

A better approximation of the experimental data is obtained with the mode depicted in eq 13 and 12 (Figure 5). Although more realistic in that histones H3 and H4 are present in the tetrameric rather than the dimeric state, this scheme calls for a rearrangement of the subunits for which there is no supportive experimental evidence (see Results). The mode fits the data fairly closely at high concentrations, but it tends to deviate from the three experimentally derived molecular weight averages at lower concentrations. Based on root mean square deviation analysis, the fit of this model is about fourfold less precise than that of the hexamer intermediate model.

Moreover, we find no evidence for the presence of the heterotypic tetramer from extensive chromatographic analysis of the core-complex peak (Eickbush & Moudrianakis, 1978). Rather, the column data are consistent with the asymmetric hexamer intermediate scheme we have proposed. Due to the reversible equilibrium between the octamer and hexamer and the similarity of their masses, the two species would be expected to coelute as a single peak on a Sephadex G-100 column (Ackers & Thompson, 1965; Cann, 1970). Furthermore, the mass ratio of the histones in the complex peak, (H3 + H4)/(H2A + H2B) = 1.28 (see Materials and Methods), is consistent with there being both octamer and hexamer present since the latter species is preferentially enriched in histones H3 and H4. A mixture of 65% octamer and 35% hexamer would give rise to the ratio found; however, a small amount of H3–H4 tetramer is undoubtedly also present in the trailing side of the peak. Because the hexamer and octamer are in reversible equilibrium, their relative concentrations (and therefore the histone ratio) should vary with column-loading concentration. Sensitivity of the histone ratio to column loading has been observed and will be described in a forthcoming paper.

The analysis of mixed-associating systems by equilibrium sedimentation presents several problems not encountered with self-associating systems. Because conserving the mass of each of the reactants is an essential factor in the mode-fitting procedure, rotor speeds must be set low enough to avoid the packing of solute on the cell bottom; if one species were to pellet preferentially, the mass balance between the reactants remaining in solution would not be the same as that of the original solution. This limitation on the rotor speed allows unambiguous analysis of only those systems whose reactants and products fall within a rather modest range of relative size. In the present study, the H2A–H2B dimer and the octamer differ in molecular weight by a factor of four. This difference seems to be close to the maximum which can be accommodated without resorting to more involved procedures (e.g., analyzing the composition of packed material on the cell bottom after the run).

We feel confident that species larger than octamer are not present in the core-complex system because of the excellent fit of the hexamer intermediate model and the absence of solute packing at equilibrium. Moreover, in the low cell-loading concentration experiments, which gave resolvable fringe patterns to the cell bottom, the total mass of the protein loaded in the cell was conserved in the solute distribution at sedimentation equilibrium; i.e.

$$\int_{r_m}^{r_b} c_r r \, dr = \int_{r_m}^{r_b} c_0 r \, dr$$

At the higher loading concentration, the fringes could not be resolved to the cell bottom; however, assuming that the fitted model is correct, c_b was estimated to be 21 mg/mL—a concentration within the solubility range of most proteins.

The conservation of the mass of the loaded solute at sedimentation equilibrium also rules out the presence, in greater than trace amounts, of dimer and species smaller than dimer at the meniscus at sedimentation equilibrium. This conclusion is supported by the presence of a gradient-free region below the meniscus at sedimentation equilibrium in both the high and low cell-loading concentration experiments. The absence of dimer at the meniscus is also predicted by the hexamer intermediate model; at both cell-loading conditions, the dimer concentration at the meniscus would be expected to be less than 0.004 mg/mL [there is no corresponding increase in the meniscus concentration with increasing c_0 because the system associates (Yphantis, 1964)]. It should be pointed out that the meniscus depletion method is particularly sensitive to the detection of low molecular weight solutes since they dominate in the very low concentration region of the distribution (Yphantis, 1964). The low-speed equilibrium sedimentation method (Van Holde & Baldwin, 1958; Teller, 1973), by contrast, is much less sensitive in this regard.

It is perhaps because they used the low-speed technique that Chung et al. (1978) were unable to detect species smaller than tetramer in their analysis of the core histone association. Furthermore, since apparent number-average molecular weights are evaluated from the relationship (Adams & Filmer, 1966)

$$M_{nc(app)} = c/\left(\int_0^c dc/M_{wc(app)}\right)$$

this method does not yield accurate apparent number-average molecular weight values for the system unless the apparent weight-average molecular weight vs. concentration curve is accurately extrapolated to its true value at $c = 0$.[4] Chung et al. (1978) extrapolated their apparent weight-average molecular weight data (lowest concentration point at ~0.6 mg/mL) to 55 000, the molecular weight of the heterotypic tetramer, which they assumed to be the smallest species present [Figure 4 in Chung et al. (1978)]. We believe that if they had obtained data in the low concentration region (as we did in our meniscus depletion studies), the extrapolation would have intercepted the ordinate at a much lower value. Consequently, they would have calculated significantly lower values

[4] Other expressions can be used to determine $M_{nc(app)}$, but all contain integrals which must be evaluated down to zero concentration.

for $M_{nc(app)}$ and the "two-species plot" [Figure 5 in Chung et al. (1978)] would not have supported the model proposed.

Nonideality, even when it can be adequately described by a single virial term, can seriously complicate the analysis of self-associating systems (Godfrey & Harrington, 1970; Teller, 1973; Roark & Yphantis, 1969). With mixed-associating systems exhibiting nonideal behavior, an additional problem arises related to the requirement that the fitted mode demonstrate conservation of solute mass. As mentioned earlier, eq 6, which relates the total mass of a solute to its concentration at any radial level in the cell, applies only to ideally behaving solutes. For modestly nonideal systems such as the core histones, this equation can be used without measurable error if the radial position (r_a) is chosen at a point close to the center of mass of the solute at sedimentation equilibrium. This choice is based on the following consideration. Near the bottom of the cell, a nonideal solute (with a positive virial coefficient) will be at a lower concentration than an ideal solute of the same molecular weight. At the low-concentration end of the solute distribution, the opposite relationship is found. Thus, in the region of the center of mass, there is a "cross-over" point at which both solutes are at equal concentration. The cross-over point is not the same for the different species present, but if r_a is chosen near the center of mass for the concentration distribution as a whole, very little error is introduced.

For systems exhibiting more than modest nonideality, demonstrating conservation of solute mass becomes a prohibitive problem. We are unaware of a way to solve this problem which does not involve tedious repetitive procedures.

A third problem encountered in the analysis of mixed systems arises from the fact that in most instances, molecular weight vs. total concentration plots from experiments at different rotor speeds or loading concentrations do not superimpose (see Figure 3). Moreover, the degree to which they do not superimpose depends on the association mode itself. This difference from the behavior of self-associating systems can make verification of reversibility a difficult task since verification can be made only after the association mode has been correctly determined. On the other hand, this mode dependence of the overlap furnishes a check on the correctness of the analysis.

Acknowledgments

We thank Dr. William F. Harrington of this department for allowing us to use his laboratory facilities for the sedimentation equilibrium experiments of this study. We especially thank David Krusch for his performance of the many computer operations required in the analysis of the data. Lastly, we thank Dr. Peter Knight and Michael Rogers for critical readings of the manuscript.

References

Ackers, G. K., & Thompson, T. E. (1965) *Proc. Natl. Acad. Sci. U.S.A. 53*, 342–349.

Adams, E. T. (1969) *Ann. N.Y. Acad. Sci. 164*, 226–244.

Adams, E. T., & Fujita, H. (1963) in *Ultracentrifugal Analysis in Theory and Experiment* (Williams, J. W., Ed.) pp 119–130, Academic Press, New York.

Adams, E. T., & Filmer, D. L. (1966) *Biochemistry 5*, 2971–2983.

Campbell, A. M., & Cotter, R. I. (1976) *FEBS Lett. 70*, 209–211.

Candido, E. P. M., & Dixon, G. H. (1972) *Proc. Natl. Acad. Sci. U.S.A. 69*, 2015–2019.

Cann, J. R. (1970) *Interacting Macromolecules*, Chapter 3, Academic Press, New York.

Chervenka, C. H. (1973) *A Manual of Methods for the Analytical Ultracentrifuge*, pp 69–72, Beckman Instruments, Inc., Palo Alto, CA.

Chun, P. W., & Kim, S. J. (1970) *J. Phys. Chem. 74*, 899–903.

Chung, S. Y., Hill, W. E., & Doty, P. (1978) *Proc. Natl. Acad. Sci. U.S.A. 75*, 1680–1684.

D'Anna, J. A., & Isenberg, I. (1973) *Biochemistry 12*, 1035–1043.

D'Anna, J. A., & Isenberg, I. (1974a) *Biochem. Biophys. Res. Commun. 61*, 343–347.

D'Anna, J. A., & Isenberg, I. (1974b) *Biochemistry 13*, 2098–2104.

DeLange, R. J., Fambrough, D. M., Smith, E. L., & Bonner, J. (1969) *J. Biol. Chem. 244*, 5669–5679.

DeLange, R. J., Hooper, J. A., & Smith, E. L. (1973) *J. Biol. Chem. 248*, 3261–3274.

Eickbush, T. H., & Moudrianakis, E. N. (1978) *Biochemistry 17*, 4955–4964.

Eisenberg, H. (1976) *Biological Macromolecules and Polyelectrolytes in Solution*, Chapter 3, Oxford University Press, London.

Felsenfeld, G. (1978) *Nature (London) 271*, 115–122.

Fujita, H. (1975) *Foundations of Ultracentrifugal Analysis*, Chapter 4, Wiley, New York.

Glover, C. V. C., & Gorovsky, M. A. (1978) *Biochemistry 17*, 5705–5713.

Godfrey, J. E. (1976) *Biophys. Chem. 5*, 285–299.

Godfrey, J. E., & Harrington, W. F. (1970) *Biochemistry 9*, 894–908.

Harrington, W. F., & Kegeles, G. (1973) *Methods Enzymol. 27*, 306–345.

Kornberg, R. D. (1974) *Science 184*, 868–871.

Milthorpe, B. K., Jeffrey, P. D., & Nichol, L. W. (1975) *Biophys. Chem. 3*, 169–176.

Nichol, L. W., & Ogston, A. G. (1965) *J. Phys. Chem. 69*, 4365–4367.

Pardon, J. F., Worcester, D. L., Wooley, J. C., Cotter, R. I., Lilly, D. M. J., & Richards, B. M. (1977) *Nucleic Acids Res. 4*, 3199–3214.

Roark, D. E., & Yphantis, D. A. (1969) *Ann. N.Y. Acad. Sci. 164*, 245–278.

Roark, D. E., Geoghegan, T. E., & Keller, G. H. (1974) *Biochem. Biophys. Res. Commun. 59*, 542–547.

Roark, D. E., Geoghegan, T. E., Keller, G. H., Matter, K. V., & Engle, R. L. (1976) *Biochemistry 15*, 3019–3025.

Teller, D. C. (1973) *Methods Enzymol. 27*, 346–441.

Teller, D. C., Horbett, T. A., Richards, E. G., & Schachman, H. K. (1969) *Ann. N.Y. Acad. Sci. 164*, 66–101.

Thomas, J. O., & Butler, P. J. G. (1977) *J. Mol. Biol. 116*, 769–781.

Van Holde, K. E., & Baldwin, R. L. (1958) *J. Phys. Chem. 62*, 734–743.

Weintraub, H., Palter, K., & Van Lente, F. (1975) *Cell 6*, 85–110.

Wold, F. (1971) *Macromolecules: Structure and Function*, Chapter 4, Prentice-Hall, Englewood Cliffs, NJ.

Wooley, J. C., Pardon, J. F., Richards, B. M., Worchester, D. L., & Campbell, A. M. (1977) *Fed. Proc., Fed. Am. Soc. Exp. Biol. 36*, 810.

Yeoman, L. C., Olson, M. O. J., Sugano, N., Jordan, J. J., Taylor, C. W., Starbuck, W. C., & Busch, H. (1972) *J. Biol. Chem. 247*, 6018–6023.

Yphantis, D. A. (1964) *Biochemistry 3*, 297–317.